Brief Communications

Optogenetic Evidence for Inhibitory Signaling from Orexin to MCH Neurons via Local Microcircuits

John Apergis-Schoute,[1] Panagiota Iordanidou,[2] Cedric Faure,[1] Sonia Jego,[4] Cornelia Schöne,[2] Teemu Aitta-Aho,[1] Antoine Adamantidis,[3,4] and Denis Burdakov[2,5]

[1]Department of Pharmacology, University of Cambridge, Cambridge, CB2 1PD, United Kingdom, [2]Division of Neurophysiology, MRC National Institute for Medical Research, London NW7 1AA, United Kingdom, [3]Neurology Department, Bern University Hospital, 3010 Bern, Switzerland, [4]Department of Psychiatry, McGill University, Montreal, QC H3A 0G4, Canada, and [5]MRC Centre for Developmental Neurobiology, King's College London, London WC2R 2LS, United Kingdom

The lateral hypothalamus (LH) is a key regulator of multiple vital behaviors. The firing of brain-wide-projecting LH neurons releases neuropeptides promoting wakefulness (orexin/hypocretin; OH), or sleep (melanin-concentrating hormone; MCH). OH neurons, which coexpress glutamate and dynorphin, have been proposed to excite their neighbors, including MCH neurons, suggesting that LH may sometimes coengage its antagonistic outputs. However, it remains unclear if, when, and how OH actions promote temporal separation of the sleep and wake signals, a process that fails in narcolepsy caused by OH loss. To explore this directly, we paired optogenetic stimulation of OH cells (at rates that promoted awakening *in vivo*) with electrical monitoring of MCH cells in mouse brain slices. Membrane potential recordings showed that OH cell firing inhibited action potential firing in most MCH neurons, an effect that required $GABA_A$ but not dynorphin receptors. Membrane current analysis showed that OH cell firing increased the frequency of fast GABAergic currents in MCH cells, an effect blocked by antagonists of OH but not dynorphin or glutamate receptors, and mimicked by bath-applied OH peptide. In turn, neural network imaging with a calcium indicator genetically targeted to MCH neurons showed that excitation by bath-applied OH peptides occurs in a minority of MCH cells. Collectively, our data provide functional microcircuit evidence that intra-LH feedforward loops may facilitate appropriate switching between sleep and wake signals, potentially preventing sleep disorders.

Key words: **GABA; hypocretin; hypothalamus; melanin-concentrating hormone; optogenetics; orexin**

Introduction

The lateral hypothalamus (LH), historically seen as a vital source of wakefulness signals, is now known to coordinate arousal, sleep, and energy balance (Sakurai, 2002; Saper et al., 2005; de Lecea, 2012; Jego and Adamantidis, 2013). It contains a heterogeneous population of neurons, including those expressing the neuropeptides orexin/hypocretin (OH) or melanin-concentrating hormone (MCH), both of which send wide projections throughout the brain (Bittencourt et al., 1992; Trivedi et al., 1998). In several respects, OH and MCH neurons exert antagonistic actions on brain state and energy balance. Deletion of OH causes inappropriate sleepiness (narcolepsy) and weight gain (Chemelli et al., 1999; Hara et al., 2001), whereas deletion of MCH or the MCH receptor 1 results in increased hyperactivity and leanness (Shimada et al., 1998; Marsh et al., 2002; Takase et al., 2014). OH cell activation produces awakening (Adamantidis et al., 2007), whereas MCH cell activation promotes REM sleep (Jego et al., 2013; Tsunematsu et al., 2014). Chronic activation of MCH cells randomly and independently of sleep state can also increase NREM sleep (Jego and Adamantidis, 2013; Konadhode et al., 2013).

In vivo recordings suggest that MCH neurons fire during REM sleep, whereas OH neurons fire during wakefulness (Hassani et al., 2009). However, bath application of OH peptides can excite MCH neurons *in vitro* (van den Pol et al., 2004; Li and van den Pol, 2006). Hypothetically, these apparently contradictory observations could be reconciled if OH cell activity had a dual effect on the MCH network. For example, excitation of some MCH cells by OH may result in coactivation of antagonist signals, which is considered useful for fine control in some systems (Smith, 1981; Baratta et al., 1988; Cui et al., 2013: Tecuapetla et al., 2014). Concurrently, OH-dependent wakefulness would be protected from sleep intrusions if most MCH neurons were inhibited by OH cell firing, through as yet unidentified circuits. These hypotheses can be directly investigated by recording from MCH cells during OH cell firing, and by examining OH peptide effects at the level of MCH cell network. Recent technological advances allow the latter to be assessed by network-level calcium imaging (Chen

Received Dec. 28, 2014; revised Feb. 3, 2015; accepted Feb. 3, 2015.

Author contributions: J.A.-S. and D.B. designed research; J.A.-S., P.I., C.F., S.J., C.S., T.A.-A., and A.A. performed research; A.A. contributed unpublished reagents/analytic tools; J.A.-S., P.I., and D.B. analyzed data; J.A.-S. and D.B. wrote the paper.

This work was supported by the Royal Society Dorothy Hodgkin Fellowship (J.A.-S.) and HFSP Young Investigator Award (RGY0076/2012 to D.B. and A.A.).

The authors declare no competing financial interests.

Correspondence should be addressed to either of the following: Denis Burdakov, MRC Centre for Developmental Neurobiology, King's College London, London WC2R 2LS, UK, E-mail: denis.burdakov@kcl.ac.uk; or Dr John Apergis-Schoute, Department of Pharmacology, University of Cambridge, Cambridge, CB2 1PD, UK. E-mail: ja451@cam.ac.uk.

DOI:10.1523/JNEUROSCI.5269-14.2015

 0270-6474/15/355435-07$15.00/0

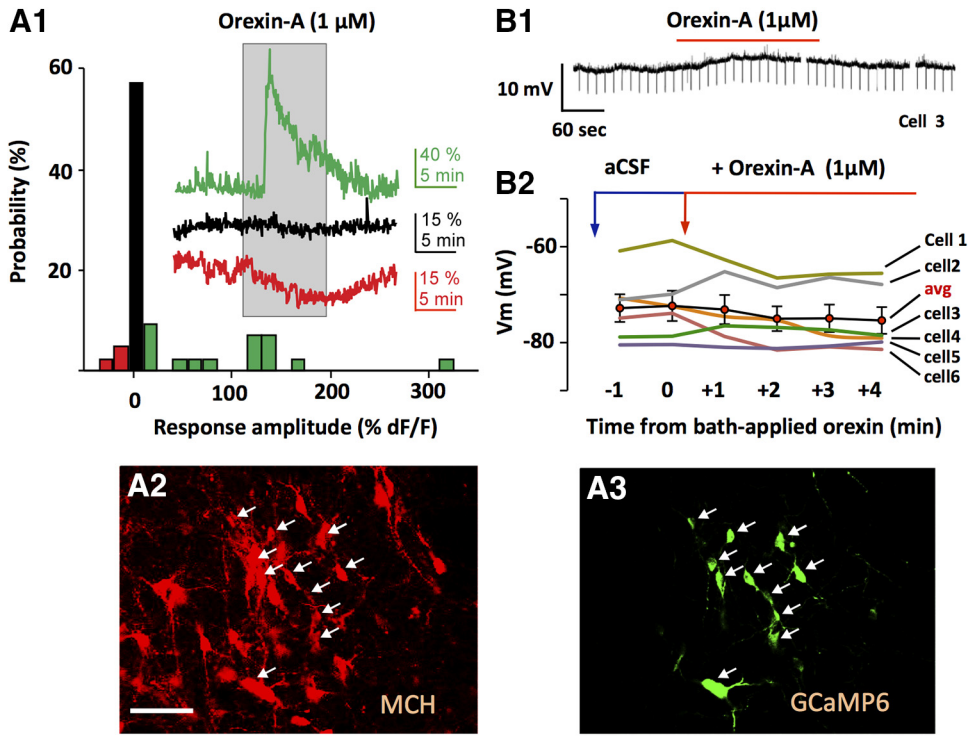

Figure 1. Responses of MCH neurons to bath-applied orexin peptide. ***A***, Summary of intracellular calcium responses of individual MCH neurons to 1 μM bath-applied orexin-A (***A1***; $n = 42$ cells). Traces show examples of excitation (green), inhibition (red), and no response (black). ***A2***,***A3***, Confirmation of localization of GCaMP6s calcium indicator to MCH neurons (see Materials and Methods). Scale bar, 80 μm. ***B***, Effect of bath applied orexin-A on MCH cell membrane potential; typical example (***B1***) and group data (***B2***).

et al., 2013), and the former by optogenetics-assisted circuit analysis (Petreanu et al., 2007). Here we apply both of these tools to explore how OH cell activity influences MCH neurons.

Materials and Methods

Gene transfer. Animal procedures followed United Kingdom Home Office regulations. AAV constructs carrying channelrhodopsin-2 (ChR2) and lentiviruses expressing mCherry under the control of MCH promoter were bilaterally stereotactically coinjected into the LH of orexin-cre mice of either sex (Matsuki et al., 2009; Sasaki et al., 2011). This targets ChR2 expression to OH neurons (Schöne et al., 2012). To target expression of mCherry to MCH neurons, we used a lentiviral vector carrying the 0.9 kb preproMCH gene promoter. The specificity of lentivirus-mediated expression was tested by stereotactic delivery of MCH::mCherry lentiviral vector ($>10^9$ pfu/ml) into the LH of MCH::eGFP transgenic mice (Stanley et al., 2010), and confirmed by staining with MCH antibody (see Fig. 2). The MCH::mCherry lentivirus used in this study was generated by Penn Vector Core, University of Pennsylvania (VSVG.HIV.MCH.mCherry(p2428), titer 3.16×10^{11} gc/ml. AAV vectors delivering ChR2 were also produced by the Penn Vector Core; we used AAV2-EF1a-DIO-ChR2(E123T/T159C)-eYFP or AAV1.EF1a.DIO.hChR2(H134R)-eYFP.WPRE.hGH. The titers of ChR2-AAVs were $>1.4 \times 10^{13}$ gc/ml. Three 100 nl injections of the mixed viruses were made at: −1.3 to −1.4 mm from bregma; ±0.9 mm from midline; and −5.30, −5.15, and −5.00 mm from skull surface. For calcium imaging, AAV carrying cre-dependent GCaMP6s (rAAV9.CAG.Flex.GCaMP6s.WPRE.SV40; Penn Vector Core, lot CS0419, titer 2.74×10^{13} gc/ml) was bilaterally stereotaxically injected into LH of MCH-cre mice (Kong et al., 2010). Three 50 nl injections of the GCaMP6s virus were at: −1.35 mm from bregma; ±0.9 mm from midline; and −5.30, −5.20, and −5.10 mm from brain surface. To confirm the selectivity of the Tg(*Pmch-Cre*) transgenic mice, animals were crossed with cre-dependent TdTomato reporter (Rosa-CAG-LSL-tdTomato-WPRE, line Ai9, Jackson Laboratories) and immunostained for MCH. 85.87 ± 1.41% of MCH-immunopositive cells were found to express TdTomato, whereas 99.81 ± 0.09% of TdTomato cells expressed MCH (2432 cells, $n = 3$ mice). GCaMP6s fluorescence was not seen after the AAV coding for GCaMP6s was injected into the LH of wild-type mice ($n = 3$ mice), confirming that it was selective to cre-containing neurons.

Calcium imaging, electrophysiology, and photostimulation. Four to six weeks after stereotactic injections, acute brain slices were prepared as in our previous work (Schöne et al., 2012). Mice were maintained on a standard 12 h light/dark cycle, and slice recordings performed in both the light (11:00 A.M. to 6:00 P.M.) and dark (6:00 P.M. to 9:00 P.M.) parts of the cycle, with similar results. For calcium imaging, brain slices were placed in a recording chamber of an upright microscope (BX61WI, Olympus) controlled by the Olympus Fluoview software (FV10-ASW ver 4.0), and perfused at 35°C with ACSF. Confocal imaging was performed at 4 Hz frame-rate through an Olympus 20× 0.50 NA objective, with a 488 nm Argon laser excitation, and 500–545 nm spectral detector emission collection. Movies were motion-corrected (StackReg plugin, ImageJ). A region of-interest (ROI) around each GCaMP6s-positive cell body was selected using the ROI manager in ImageJ. The ROI locations were used to extract the mean fluorescence value for each object on each frame $F(t)$. To correct for background activity and normalize for the fluorescence value of each cell, we first separated experimental trials into two parts: a baseline period corresponding to all the frames recorded before one frame after the presentation of orexin, and a stimulus period, beginning 4 s after the onset of orexin application and lasting 10 min. Next, for each ROI we calculated $\%dF/F$ for each frame (t), where $dF/F = (F(t) - F)$ *100/F, and F was the mean fluorescence value for that ROI for all frames in the baseline period for that trial. For whole-cell patch-clamp recordings, performed and analyzed as in our previous work (Schöne et al., 2012), MCH cells were visualized in acute living brain slices using a mCherry filter set (Chroma). To stimulate ChR2, we used a Thorlabs blue LED, delivering ~10 mW/mm^2 light to ChR2-containing axons around the recorded cell through a 40× 0.8 NA objective. Whole-cell recordings were performed at 37°C using an EPC-10 amplifier and Patch-Master software (HEKA Elektronik). Averaged data are presented as the mean ± SEM. Statistical significance was evaluated using ANOVA with Bonferonni post-test, unless stated otherwise.

Chemicals and solutions. Slice-cutting and recording ACSF was gassed with 95% O_2 and 5% CO_2, and contained the following (mM): 125 NaCl,

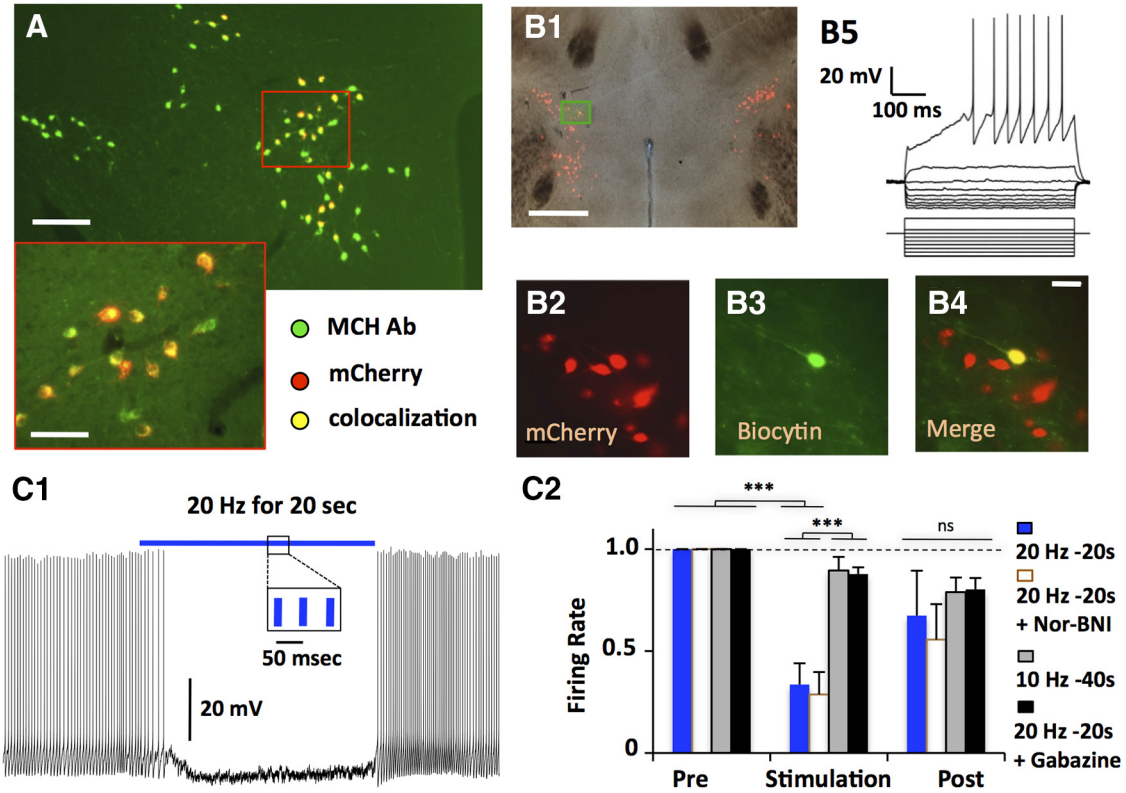

Figure 2. Membrane potential effects in MCH neurons of activation of intrinsic OH neurons. ***A***, Targeted expression of mCherry in MCH neurons ($n = 3$ animals, 630/638 mCherry cells colocalised with MCH). Scale bars: top, 200 μm; inset, 40 μm. ***B***, Whole-cell recordings in mCherry-expressing neurons (***B2***) were confirmed by filling neurons with biocytin (***B3***, ***B4***). Membrane potential responses to current injections (***B5***); $n = 50$ cells. ***C***, Effect of optogenetic stimulation of OH neurons. Typical example (***C1***) and summary of effects of different stimulation frequencies and drug conditions on firing rate, normalized to prestimulation firing (***C2***); $n = 7$ cells, two-way ANOVA, $F_{(2,42)} = 21.37$, Bonferroni post-test; ***$p < 0.001$; ns, nonsignificant ($p > 0.05$).

25 $NaHCO_3$, 3 KCl, 1.25 NaH_2PO_4, 1/2 $CaCl_2$ (cutting/recording), 6/1 $MgCl_2$ (cutting/recording), 3 sodium pyruvate, and 25/5 glucose (cutting/recording). Pipettes were filled with (in mM): 135 potassium gluconate, 7 NaCl, 10 HEPES, 2 Na_2-ATP, 0.3 Na-GTP, and 2 $MgCl_2$; pH was adjusted to 7.3 with KOH. Drug concentrations were (in μm): 20 CNQX and 100 AP5, 10 gabazine, 1 TTX, 5 nor-binaltorphimine dihydrochloride (nor-BNI), 10 SB-334867 (SB), and 10 TCS-OX2–29 (TCS). All chemicals were from Signal, Tocris Bioscience, or Bachem.

Immunocytochemistry. Primary antibodies were as follows: goat anti-orx-B (1:1000; Santa Cruz Biotechnology), rabbit anti-GABA (1:500; Immunostar), and rabbit anti-MCH (1:1000, Phoenix Pharmaceuticals) Secondary antibodies were AlexaFluor 594 donkey anti-rabbit and AlexaFluor 488 donkey anti-goat (both 1:1000; Thermo Fisher). Orexin, MCH, and biocytin immunostaining was performed as in our previous work (Burdakov et al., 2005). For GABA immunostaining, tissue was heated to 80°C for 30 min in sodium citrate (pH 8; Sigma-Aldrich), washed in 0.1 M PBS, treated three times for 5 min in sodium borohydride solution (1 mg/ml in PBS), again washed in 0.1 M PBS, and blocked/permeabilized in PBS with 0.3% Triton X-100 (Sigma-Aldrich) and 5% donkey serum (Sigma-Aldrich). Sections were then incubated overnight in blocking solution with rabbit anti-GABA and goat anti-orx-B. On Day 2, tissue was washed in 0.1 M PBS, incubated in secondary antibodies for 2 h, washed in PBS, and mounted on microscope slides and coverslipped. Digital images were captured with a Zeiss Axioskop 2 microscope and QImaging QICAM Fast digital camera. Images were merged using ImageJ (National Institutes of Health). Expression was analyzed separately and subsequently merged and counted manually.

Results

Artificially applied orexin/hypocretin excites a minor part of the MCH network

To explore OH peptide effects on MCH network, we first targeted genetically encoded calcium indicators selectively to MCH neurons in MCH-cre transgenic mice (see Materials and Methods; Fig. 1*A*). This allows monitoring of neuronal excitation by using cytosolic calcium concentration as a proxy (Chen et al., 2013). In this assay, ~30% of MCH neurons were activated by 1 μM bath-applied orexin-A; the rest were either unaffected or inhibited (Fig. 1*A*). Second, we performed whole-cell current-clamp recordings, where bath application of 1 μM orexin-A also had mixed effects on MCH cell membrane potential: some MCH neurons slightly depolarized, but others were hyperpolarized or did not respond (2/6 and 4/6 cells, respectively; Fig. 1*B*). These results are consistent with previous work showing that some MCH neurons can be activated by 1 μM artificially applied orexin (van den Pol et al., 2004; Li and van den Pol, 2006), but our data suggest that this activation occurs in a minority of MCH cells.

Firing of OH neurons exerts inhibitory effects on MCH cell membrane potential

Artificial application of neurotransmitters involves arbitrarily chosen concentrations that may not correspond to those in native neural networks, potentially creating unnatural responses (e.g., due to receptor desensitization). To examine intrinsic signals generated by OH cell firing in MCH neurons, we performed optogenetic analysis of functional connectivity in LH brain slices. To selectively stimulate OH cells while recording from identified MCH cells, we expressed light-activated excitatory ion channel ChR2 in OH neurons and simultaneously transduced MCH neurons using lentiviral vector expressing the mCherry fluorescent protein driven by an MCH gene promoter (Fig. 2*A*; see Materials and Methods). Following stereotaxic injections of the mCherry-MCH lentiviruses into the LH, mCherry-labeled neurons were

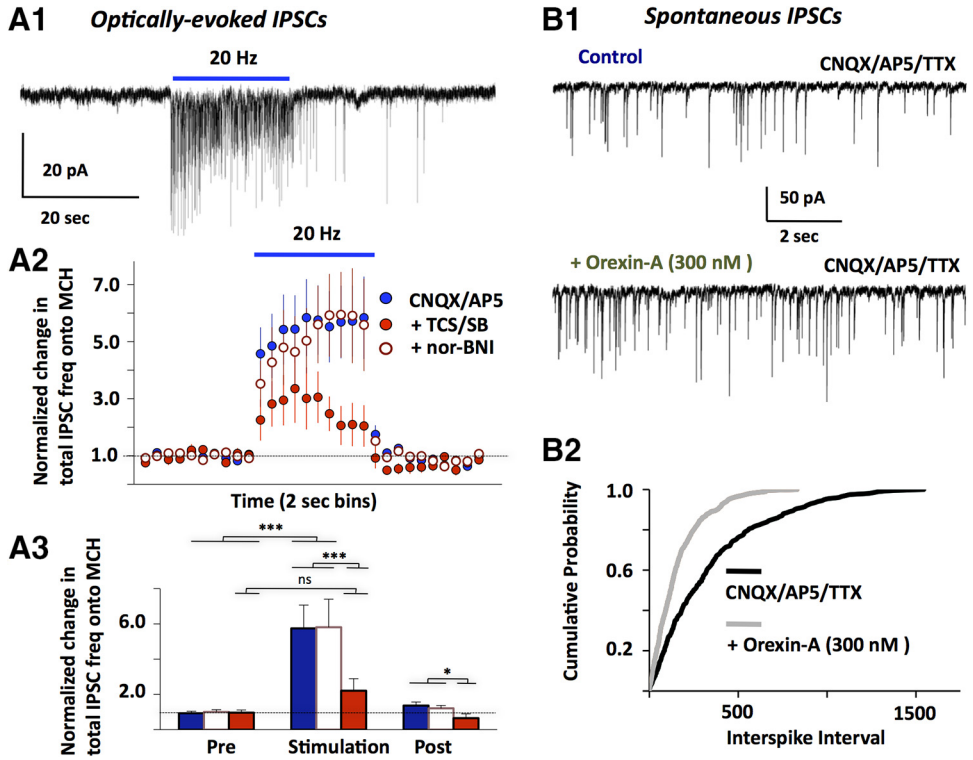

Figure 3. Membrane current effects in MCH neurons of activating intrinsic OH neurons, and of bath-applied OH peptide. ***A1***, Typical example of MCH cell IPSCs caused by optical stimulation of OH cells ($n = 26$ cells). IPSCs were recorded in the presence of CNQX/AP5, and confirmed as GABAergic by blockade with gabazine. ***A2***, Summary of effects of OH cell stimulation on MCH cell IPSC tone, under different drug conditions ($n = 26$ cells). ***A3***, Comparison of IPSC tone at different times relative to the optical stimulation (6 s before, last 6 s of stimulation, and 6 s after the stimulation). Color codes and data are the same as in ***A2***. Two-way ANOVA, $F_{(2,42)} = 21.37$, Bonferroni post-test: ***$p < 0.001$; *$p < 0.05$; ns, nonsignificant ($p > 0.05$). ***B1***, Typical example of effect of bath applied orexin-A on miniature IPSCs ($n = 5$ cells). ***B2***, Comparison of miniature IPSC frequency with and without bath orexin; $n = 5$ cells, Kolmogorov–Smirnov test, $p < 0.001$.

found only in the previously reported locations of MCH neurons (the Zona Incerta, Lateral and Dorsomedial Hypothalamus; Fig. 2*A*,*B1*). MCH-like immunoreactivity was found in 98.7% of mCherry-labeled cells (Fig. 2*A*; statistics for data shown in the figures are reported in figure legends). Whole-cell recordings from the mCherry cells (Fig. 2*B5*) revealed typical membrane potential "signatures" of MCH cells (Burdakov et al., 2005), confirming that MCH cell function was unperturbed by the viral infection. The firing of most MCH-mCherry cells was rapidly reduced when OH-ChR2 cells were optically paced at a frequency that we previously found to cause awakening *in vivo* (20 Hz; Adamantidis et al., 2007; Fig. 2*C*; $n = 25/32$ cells; note that this represents ≈80% of MCH cells with only ≈40% of OH cells transfected with ChR2 in our preparation; Schöne et al., 2012). Lower optical stimulation frequencies were less effective (Fig. 2*C2*), mirroring stimulation requirement for OH peptide release in slices (Schöne et al., 2014). Dynorphin is coexpressed in OH neurons (Muschamp et al., 2014), and extrinsic application of dynorphin can inhibit MCH neurons via κ-opiod receptors (Li and van den Pol, 2006). However, the κ-opiod receptor antagonist Nor-BNI did not affect the inhibition of MCH activity by OH cell firing (Fig. 2*C2*). In contrast, the OH → MCH inhibition was largely abolished by 10 μM gabazine, a $GABA_A$ receptor blocker, suggesting that it is mediated by local GABA release (Fig. 2*C2*).

OH cell firing controls GABA input to MCH cells via OH receptors

To further investigate synaptic currents underlying the GABAergic suppression of MCH cell activity during OH cell firing, we performed voltage-clamp recordings (at −80 mV) in glutamate receptor blockers (CNQX+AP5). Optical stimulation significantly increased the frequency of gabazine-sensitive IPSCs (Fig. 3*A*). IPSC frequency increased progressively during optical stimulation (Fig. 3*A2*), similar to actions of OH peptides expected to be released by this stimulation (Schöne et al., 2014). Application of OH receptor antagonists substantially reduced the ability of the optical stimulation to increase GABAergic tone (Fig. 3*A*). In contrast, κ-opiod receptor antagonist did not affect the IPSC stimulation (Fig. 3*A2*,*3*). If our optical stimulation increases GABA input to MCH cells by releasing endogenous OH peptides, then the increase in GABAergic tone should be mimicked by artificially applied OH peptides. Indeed, bath-applied OH peptide significantly increased the frequency of miniature $GABA_A$-mediated IPSCs (Fig. 3*B*).

Interestingly, in some cases we observed $GABA_A$-mediated IPSCs in MCH neurons that appeared time-locked (2–10 ms latency) to the optical flashes stimulating OH neurons (Fig. 4*A*). The probability of the short-latency (<10 ms) IPSCs was also increased by bath-applied OH peptide (Fig. 4*A3*). It has been suggested that latencies >1.8 ms may represent indirect, polysynaptic connections (Gil and Amitai, 1996). Thus, our latencies could mean that OH neurons fire GABA interneurons projecting to MCH cells, presumably by releasing OH peptide since the responses persisted in glutamate receptor blockers (Fig. 4*A1*). Alternatively, due to delays between optical flashes and the spikes they evoke in ChR2-expressing cells (Tecuapetla et al., 2010), it cannot be excluded that some OH cells may release GABA onto MCH cells. Indeed, it has been previously hypothesized based on immunocytochemistry, real-time PCR, and electron-microscopy that a subgroup of

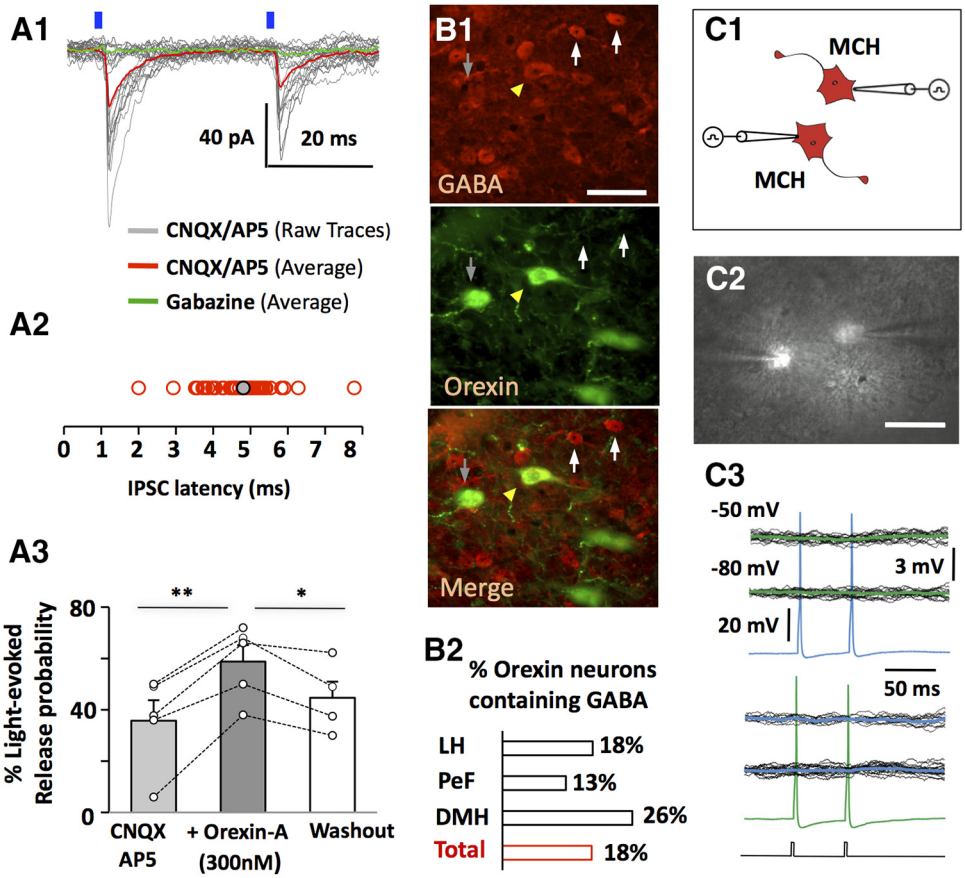

Figure 4. Inhibitory actions and GABA content of OH neurons. ***A1***, An example of a short-latency (<10 ms) IPSC evoked by a blue laser flashes ($n = 7$ cells). ***A2***, distribution of short latencies (***A2***; $n = 48$ cells). ***A3***, effect on bath-applied orexin-A on short-latency IPSC recorded as in ***A1*** ($n = 5$ cells). Paired two-tailed Student's t test, $^{**}p < 0.005$, $^{*}p < 0.05$; ns, nonsignificant ($p > 0.05$). ***B***, Orexin-containing neurons immunopositive for GABA (***B1***) are distributed throughout hypothalamic subregions. The number of OH-immunopositive cells colocalized with GABA were as follows: LH, 107/590; perifornical area (PeF), 23/88; dorsomedial hypothalamus (DMH), 29/226; total 159/908 cells ($n = 3$ brains; ***B2***). Scale bar, 40 μm. ***C***, Schematic (***C1***) and live brain-slice image (***C2***) of paired recordings from MCH-mCherry neurons. Scale bar, 50 μm. ***C3***, representative recordings from an MCH-MCH cell pair, showing that evoked action potentials in one cell did not produce postsynaptic current in the other. Black lines are individual traces and green/blue are averaged traces. Current-clamp protocol used to evoke action potentials is shown below the traces. Similar results were obtained from 43 cell pairs.

OH cells may release GABA (Guan et al., 2002; Harthoorn et al., 2005; Balcita-Pedicino and Sesack, 2007). We confirmed that GABA-like immunoreactivity is present in a subpopulation of OH neurons (10–25% of OH cells, depending on LH area; Fig. 4*B*, but see Discussion).

At least some MCH cells are GABAergic (Jego et al., 2013), and some may be excited by OH neurons (Fig. 1*A1*; Guan et al., 2002; van den Pol et al., 2004; Li and van den Pol, 2006). This suggests a possibility that some of OH-dependent GABA drive to MCH neurons may come from other MCH neurons. To test this, we performed dual whole-cell recordings from identified MCH-mCherry cell pairs (Fig. 4*C*). We generated action potentials in one MCH cell, while recording synaptic responses in another MCH cell. We did not find evidence of MCH-to-MCH functional connectivity: presynaptic action potentials did not generate detectable postsynaptic responses in 43 MCH-MCH cell pairs tested (Fig. 4*C*).

Discussion

A key question in systems neuroscience is how the brain ensures that opposing signals, such those causing sleep and wake transitions, are scheduled to occur at separate times. Inappropriate co-occurrence of such signals can produce pathological brain states and behaviors, for example concurrent wakefulness and sleep-paralysis (Dauvilliers et al., 2007). Our results provide a network-level explanation for how such pathological mixing of opposing neural drives may be prevented by natural LH microcircuits. Our data suggest that when OH neurons fire at rates that promote awakening (Adamantidis et al., 2007), the spike output of most MCH neurons is suppressed, due to increased GABAergic drive into those cells (Fig. 2*C*). The GABAergic inhibition of MCH cells depends significantly on OH receptors, whereas glutamate receptors are not essential (Fig. 3*A2*). This is consistent with our previous data that OH (but not glutamate) transmission is critical for translating OH cell firing into sustained postsynaptic electrical responses (Schöne et al., 2014). Our data are also consistent with the possibility that OH may release GABA themselves (Fig. 4). However, further molecular and ultra-structural data would be necessary to ascertain how OH cells may produce GABA and/or package it into vesicles, because the GABA staining we observed may be cytosolic (and not vesicular), and we found no evidence of OH immunoreactivity in vgat-positive neurons of the LH (D. Burdakov and J. Apergis-Schoute, unpublished observations). It remains to be determined whether OH neurons may acquire GABAergic functional identity through noncanonical transporters, such as recently reported for dopamine neurons (Tritsch et al., 2012, 2014).

More broadly, our results offer a reconciliation for the apparent contradictions in existing *in vitro* and *in vivo* data on relative timing of OH and MCH cell activity (van den Pol et al., 2004; Hassani et al., 2009). Although we observed only inhibitory effects during intrinsic OH cell → MCH cell actions (consistent with Hassani et al., 2009), our data with bath applications of OH peptide suggested that it may also directly excite some MCH neurons (consistent with van den Pol et al., 2004). It is possible that the high levels of OH peptide required to excite MCH cells are not attained during optogenetic stimulation in slices or during acute experiments. *In vivo*, during overexcitation of OH cells, it remains possible that OH peptides may reach high-enough levels to excite MCH cells directly, which may provide a feedback mechanism preventing hyperarousal. In terms of natural drives of OH neurons, there is evidence that noradrenaline input to OH cells may switch sign after sleep deprivation due to a switch in receptor type (Grivel et al., 2005; Uschakov et al., 2011). This suggests the coupling of MCH cell activity to arousal state in general, and to noradrenaline drive in particular, may change as a function of stress or sleep pressure, an interesting possibility that deserves future investigation.

We predict that the OH receptor-dependent intrinsic OH → MCH inhibitory signaling (Fig. 3*A2*) is mediated by local OH-excited GABA neurons. It would be important to determine the identities of these neurons in future investigations, and our paired recordings (Fig. 4*C*) currently suggest that these GABA cells may be separate from MCH neurons themselves. At the level of local circuits in the LH, our data provide functional experimental support for the "flip-flop" model of binary switching between sleep and wake signals (Saper et al., 2005). The GABAergic microcircuits mediating OH → MCH cell inhibition may constitute a new therapeutic target, because they are likely to oppose the pathological mixing of sleep and wake states in disorders such as narcopelsy.

References

Adamantidis AR, Zhang F, Aravanis AM, Deisseroth K, de Lecea L (2007) Neural substrates of awakening probed with optogenetic control of hypocretin neurons. Nature 450:420–424. CrossRef Medline

Balcita-Pedicino JJ, Sesack SR (2007) Orexin axons in the rat ventral tegmental area synapse infrequently onto dopamine and gamma-aminobutyric acid neurons. J Comp Neurol 503:668–684. CrossRef Medline

Baratta R, Solomonow M, Zhou BH, Letson D, Chuinard R, D'Ambrosia R (1988) Muscular coactivation: the role of the antagonist musculature in maintaining knee stability. Am J Sports Med 16:113–122. CrossRef Medline

Bittencourt JC, Presse F, Arias C, Peto C, Vaughan J, Nahon JL, Vale W, Sawchenko PE (1992) The melanin-concentrating hormone system of the rat brain: an immuno- and hybridization histochemical characterization. J Comp Neurol 319:218–245. CrossRef Medline

Burdakov D, Gerasimenko O, Verkhratsky A (2005) Physiological changes in glucose differentially modulate the excitability of hypothalamic melanin-concentrating hormone and orexin neurons in situ. J Neurosci 25:2429–2433. CrossRef Medline

Chemelli RM, Willie JT, Sinton CM, Elmquist JK, Scammell T, Lee C, Richardson JA, Williams SC, Xiong Y, Kisanuki Y, Fitch TE, Nakazato M, Hammer RE, Saper CB, Yanagisawa M (1999) Narcolepsy in orexin knockout mice: molecular genetics of sleep regulation. Cell 98:437–451. CrossRef Medline

Chen TW, Wardill TJ, Sun Y, Pulver SR, Renninger SL, Baohan A, Schreiter ER, Kerr RA, Orger MB, Jayaraman V, Looger LL, Svoboda K, Kim DS (2013) Ultrasensitive fluorescent proteins for imaging neuronal activity. Nature 499:295–300. CrossRef Medline

Cui G, Jun SB, Jin X, Pham MD, Vogel SS, Lovinger DM, Costa RM (2013) Concurrent activation of striatal direct and indirect pathways during action initiation. Nature 494:238–242. CrossRef Medline

Dauvilliers Y, Arnulf I, Mignot E (2007) Narcolepsy with cataplexy. Lancet 369:499–511. CrossRef Medline

de Lecea L (2012) Hypocretins and the neurobiology of sleep–wake mechanisms. Prog Brain Res 198:15–24. CrossRef Medline

Gil Z, Amitai Y (1996) Properties of convergent thalamocortical and intracortical synaptic potentials in single neurons of neocortex. J Neurosci 16:6567–6578. Medline

Grivel J, Cvetkovic V, Bayer L, Machard D, Tobler I, Mühlethaler M, Serafin M (2005) The wake-promoting hypocretin/orexin neurons change their response to noradrenaline after sleep deprivation. J Neurosci 25:4127–4130. CrossRef Medline

Guan JL, Uehara K, Lu S, Wang QP, Funahashi H, Sakurai T, Yanagizawa M, Shioda S (2002) Reciprocal synaptic relationships between orexin- and melanin-concentrating hormone-containing neurons in the rat lateral hypothalamus: a novel circuit implicated in feeding regulation. Int J Obes Relat Metab Disord 26:1523–1532. CrossRef Medline

Hara J, Beuckmann CT, Nambu T, Willie JT, Chemelli RM, Sinton CM, Sugiyama F, Yagami K, Goto K, Yanagisawa M, Sakurai T (2001) Genetic ablation of orexin neurons in mice results in narcolepsy, hypophagia, and obesity. Neuron 30:345–354. CrossRef Medline

Harthoorn LF, Sañé A, Nethe M, Van Heerikhuize JJ (2005) Multitranscriptional profiling of melanin-concentrating hormone and orexin-containing neurons. Cell Mol Neurobiol 25:1209–1223. CrossRef Medline

Hassani OK, Lee MG, Jones BE (2009) Melanin-concentrating hormone neurons discharge in a reciprocal manner to orexin neurons across the sleep–wake cycle. Proc Natl Acad Sci U S A 106:2418–2422. CrossRef Medline

Jego S, Adamantidis A (2013) MCH neurons: vigilant workers in the night. Sleep 36:1783–1786. CrossRef Medline

Jego S, Glasgow SD, Herrera CG, Ekstrand M, Reed SJ, Boyce R, Friedman J, Burdakov D, Adamantidis AR (2013) Optogenetic identification of a rapid eye movement sleep modulatory circuit in the hypothalamus. Nat Neurosci 16:1637–1643. CrossRef Medline

Konadhode RR, Pelluru D, Blanco-Centurion C, Zayachkivsky A, Liu M, Uhde T, Glen WB Jr, van den Pol AN, Mulholland PJ, Shiromani PJ (2013) Optogenetic stimulation of MCH neurons increases sleep. J Neurosci 33:10257–10263. CrossRef Medline

Kong D, Vong L, Parton LE, Ye C, Tong Q, Hu X, Choi B, Brüning JC, Lowell BB (2010) Glucose stimulation of hypothalamic MCH neurons involves K(ATP) channels, is modulated by UCP2, and regulates peripheral glucose homeostasis. Cell Metab 12:545–552. CrossRef Medline

Li Y, van den Pol AN (2006) Differential target-dependent actions of coexpressed inhibitory dynorphin and excitatory hypocretin/orexin neuropeptides. J Neurosci 26:13037–13047. CrossRef Medline

Marsh DJ, Weingarth DT, Novi DE, Chen HY, Trumbauer ME, Chen AS, Guan XM, Jiang MM, Feng Y, Camacho RE, Shen Z, Frazier EG, Yu H, Metzger JM, Kuca SJ, Shearman LP, Gopal-Truter S, MacNeil DJ, Strack AM, MacIntyre DE, et al. (2002) Melanin-concentrating hormone 1 receptor-deficient mice are lean, hyperactive, and hyperphagic and have altered metabolism. Proc Natl Acad Sci U S A 99:3240–3245. CrossRef Medline

Matsuki T, Nomiyama M, Takahira H, Hirashima N, Kunita S, Takahashi S, Yagami K, Kilduff TS, Bettler B, Yanagisawa M, Sakurai T (2009) Selective loss of GABA(B) receptors in orexin-producing neurons results in disrupted sleep/wakefulness architecture. Proc Natl Acad Sci U S A 106:4459–4464. CrossRef Medline

Muschamp JW, Hollander JA, Thompson JL, Voren G, Hassinger LC, Onvani S, Kamenecka TM, Borgland SL, Kenny PJ, Carlezon WA Jr (2014) Hypocretin (orexin) facilitates reward by attenuating the antireward effects of its cotransmitter dynorphin in ventral tegmental area. Proc Natl Acad Sci U S A 111:E1648–E1655. CrossRef Medline

Petreanu L, Huber D, Sobczyk A, Svoboda K (2007) Channelrhodopsin-2-assisted circuit mapping of long-range callosal projections. Nat Neurosci 10:663–668. CrossRef Medline

Sakurai T (2002) Role of orexins in the regulation of feeding and arousal. Sleep Med 3:S3–S9. CrossRef Medline

Saper CB, Scammell TE, Lu J (2005) Hypothalamic regulation of sleep and circadian rhythms. Nature 437:1257–1263. CrossRef Medline

Sasaki K, Suzuki M, Mieda M, Tsujino N, Roth B, Sakurai T (2011) Pharmacogenetic modulation of orexin neurons alters sleep/wakefulness states in mice. PLoS One 6:e20360. CrossRef Medline

Schöne C, Cao ZF, Apergis-Schoute J, Adamantidis A, Sakurai T, Burdakov D (2012) Optogenetic probing of fast glutamatergic transmission from

hypocretin/orexin to histamine neurons in situ. J Neurosci 32:12437–12443. CrossRef Medline

Schöne C, Apergis-Schoute J, Sakurai T, Adamantidis A, Burdakov D (2014) Coreleased orexin and glutamate evoke nonredundant spike outputs and computations in histamine neurons. Cell Rep 7:697–704. CrossRef Medline

Shimada M, Tritos NA, Lowell BB, Flier JS, Maratos-Flier E (1998) Mice lacking melanin-concentrating hormone are hypophagic and lean. Nature 396:670–674. CrossRef Medline

Smith AM (1981) The coactivation of antagonist muscles. Can J Physiol Pharmacol 59:733–747. CrossRef Medline

Stanley S, Pinto S, Segal J, Pérez CA, Viale A, DeFalco J, Cai X, Heisler LK, Friedman JM (2010) Identification of neuronal subpopulations that project from hypothalamus to both liver and adipose tissue polysynaptically. Proc Natl Acad Sci U S A 107:7024–7029. CrossRef Medline

Takase K, Kikuchi K, Tsuneoka Y, Oda S, Kuroda M, Funato H (2014) Meta-analysis of melanin-concentrating hormone signaling-deficient mice on behavioral and metabolic phenotypes. PLoS One 9:e99961. CrossRef Medline

Tecuapetla F, Patel JC, Xenias H, English D, Tadros I, Shah F, Berlin J, Deisseroth K, Rice ME, Tepper JM, Koos T (2010) Glutamatergic signaling by mesolimbic dopamine neurons in the nucleus accumbens. J Neurosci 30:7105–7110. CrossRef Medline

Tecuapetla F, Matias S, Dugue GP, Mainen ZF, Costa RM (2014) Balanced activity in basal ganglia projection pathways is critical for contraversive movements. Nat Commun 5:4315. CrossRef Medline

Tritsch NX, Ding JB, Sabatini BL (2012) Dopaminergic neurons inhibit striatal output through non-canonical release of GABA. Nature 490:262–266. CrossRef Medline

Tritsch NX, Oh WJ, Gu C, Sabatini BL (2014) Midbrain dopamine neurons sustain inhibitory transmission using plasma membrane uptake of GABA, not synthesis. Elife 3:e01936. CrossRef Medline

Trivedi P, Yu H, MacNeil DJ, Van der Ploeg LH, Guan XM (1998) Distribution of orexin receptor mRNA in the rat brain. FEBS Lett 438:71–75. CrossRef Medline

Tsunematsu T, Ueno T, Tabuchi S, Inutsuka A, Tanaka KF, Hasuwa H, Kilduff TS, Terao A, Yamanaka A (2014) Optogenetic manipulation of activity and temporally controlled cell-specific ablation reveal a role for MCH neurons in sleep/wake regulation. J Neurosci 34:6896–6909. CrossRef Medline

Uschakov A, Grivel J, Cvetkovic-Lopes V, Bayer L, Bernheim L, Jones BE, Mühlethaler M, Serafin M (2011) Sleep-deprivation regulates alpha-2 adrenergic responses of rat hypocretin/orexin neurons. PLoS One 6:e16672. CrossRef Medline

van den Pol AN, Acuna-Goycolea C, Clark KR, Ghosh PK (2004) Physiological properties of hypothalamic MCH neurons identified with selective expression of reporter gene after recombinant virus infection. Neuron 42:635–652. CrossRef Medline